HHS Public Access

Author manuscript

Conf Proc IEEE Eng Med Biol Soc. Author manuscript; available in PMC 2020 July 01.

Published in final edited form as:

Conf Proc IEEE Eng Med Biol Soc. 2019 July ; 2019: 2852–2855. doi:10.1109/EMBC.2019.8856503.

Development of a Physiologically-Based Mathematical Model for Quantifying Nanoparticle Distribution in Tumors

Prashant Dogra,
Mathematics in Medicine Program, Houston Methodist Research Institute, Houston, TX 77030, USA

Yao-li Chuang,
Department of Mathematics, California State University, Northridge, CA 91330, USA.

Joseph D. Butner,
Mathematics in Medicine Program, Houston Methodist Research Institute, Houston, TX 77030, USA

Vittorio Cristini,
Mathematics in Medicine Program, Houston Methodist Research Institute, Houston, TX 77030, USA.

Department of Imaging Physics, University of Texas MD Anderson Cancer Center, Houston, TX 77230, USA

Zhihui Wang [Member, IEEE]
Mathematics in Medicine Program, Houston Methodist Research Institute, Houston, TX 77030, USA.

Department of Imaging Physics, University of Texas MD Anderson Cancer Center, Houston, TX 77230, USA

Abstract

Nanomedicine holds promise for the treatment of cancer, as it enables tumor-targeted drug delivery. However, reports on translation of most nanomedicine strategies to the clinic so far have been less than satisfactory, in part due to insufficient understanding of the effects of nanoparticle (NP) physiochemical properties and physiological variables on their pharmacological behavior. In this paper, we present a multiscale mathematical model to examine the efficacy of NP delivery to solid tumors; as a case example, we apply the model to a clinically detectable primary pancreatic ductal adenocarcinoma (PDAC) to assess tissue-scale spatiotemporal distribution profiles of NPs. We integrate NP systemic disposition kinetics with NP-cell interactions in PDAC abstractly described as a two-dimensional structure, which is then parameterized with human physiological data obtained from published literature. Through model analysis of delivery efficiency, we verify the multiscale approach by showing that NP concentration kinetics of interest in various compartments predicted by the whole-body scale model were in agreement with those obtained from the tissue-scale model. We also found that more NPs were trapped in the outer well-perfused

(corresponding author, zwang@houstonmethodist.org).

tumor region than the inner semi-necrotic domain. Further development of the model may provide a useful tool for optimal NP design and physiological interventions.

I. Introduction

Chemotherapy, the mainstay of preoperative intervention for cancer patients in the clinic, is often associated with side effects, such as off-target cytotoxicity and drug resistance [1, 2]. It has been reported that encapsulating cytotoxic agents in nanoparticles (NPs) has the potential to improve the low therapeutic index of these agents [3]. Tumor vasculature is known to be leaky due to microscopic inter-endothelial gaps in the malformed neovasculature, which allows for increased NP accumulation in the tumor interstitium through the enhanced permeability and retention (EPR) effect [4], thus providing passive targeting to deliver the cytotoxic cargo to the tumor. Alternatively, by functionalizing the surface of NPs with ligands specific to receptors in the tumor tissue, NPs can be actively targeted to deliver the loaded drugs to the tumor [5]. These delivery strategies, developed based on unique tumor features, are thought to reduce drug exposure to non-target sites.

However, only limited success has been achieved in the clinical translation of cancer nanotherapy [6]. In a recent meta-analysis report [7], on average only 0.7% of the injected dose of NPs is successfully delivered to a tumor. In addition to Kupffer cells in liver and macrophages in spleen, fenestrated and sinusoidal endothelial capillaries in these and other organs contribute to NP sequestration through healthy tissues. For example, fenestrated endothelial capillaries in kidneys and pancreas [8] permit NP accumulation based on the relative size between NPs and pores in such capillaries. On the contrary, in organs with continuous endothelial capillaries (e.g., heart, lungs) [8], NPs are generally beyond the filtration limit of the capillary wall pores, and negligible accumulation occurs in these locations. Thus, physiological features like blood vessel wall pores and macrophages (referred to as *traps* in this paper) are likely the drivers of global NP biodistribution in the body. It has also been demonstrated that NP physicochemical properties, such as size, surface charge, and surface chemistry, also play a key role in tailoring NP biodistribution and clearance behavior [9]. The complex interplay between NP properties and anatomical features at the microscopic scale determines the macroscopic behavior of NPs, and mathematical models may provide a useful and tractable tool to study this phenomena.

Mathematical modeling has been extensively used in mechanistically explaining the observed data and in deriving new experimentally and/or clinically testable predictions in many cancer research fields [10–23]. In cancer nanomedicine, previous mathematical models have revealed valuable insights into the *in vivo* dynamics of NPs [24]. Mechanistic models at the cellular scale [25] have explained the NP-cellular interactions responsible for NP phagocytosis and endothelial cell adhesion, as well as the effects of NP physicochemical properties on these interactions. Computational fluid dynamics models at the single capillary scale have provided theoretical understanding of critical phenomenon, such as NP margination or lateral drift towards the vessel wall [26], and the effects of hematocrit, particle size, and shape on the intravascular behavior of NPs. Tissue-scale models [27] have examined the effects of NP properties and tumor pathophysiology on active and passive

delivery of NPs to the tumor. Lastly, at the whole-body scale, NP biodistribution and clearance have been studied by employing physiologically based pharmacokinetic (PBPK) modeling [28, 29]. All these modeling approaches, while providing valuable understanding of the processes involved in NP biodistribution, generally focus on one spatial scale at a time and assume prescribed information from other scales as fixed properties, despite NP-mediated drug delivery to tumors being a multiscale, multi-step dynamical processes.

A modeling framework that integrates multiple relevant scales can improve the predictive power of mathematical models to examine *in silico* the effects of various particle- and tissue-related properties (variables) on the biological behavior of NPs, generating experimentally testable hypotheses for NP design and physiological interventions. To this end, we present an integrative mathematical model that spans across multiple scales (i.e., whole-body, tissue, and cellular scales) to study the delivery and spatiotemporal distribution of NPs in a solid tumor.

II. Model development

We have developed a multiscale physiologically-based model, composed of sub-models at three different spatiotemporal scales: whole-body, tissue, and cell scales, as illustrated in Fig. 1. We briefly discuss the development of the main modeling components on each scale below.

A. Whole-body scale

To describe the macroscopic exposure of tumor and its host organ to the injected NPs, we use a whole-body PBPK modeling approach [30] to determine the systemic blood concentration kinetics of NPs. To take an initial step towards the multiscale approach, in this paper we retain only the most essential driving mechanisms of NP systemic circulation kinetics, and include only systemic circulation, liver, and kidney compartments in the PBPK model. We use a standard approach based on ordinary differential equations (ODEs) for modeling free-flowing NP concentration in each compartment, such that free flowing NPs = Incoming NPs – Outgoing NPs –Trapped NPs.

B. Tissue and cell scales

We employ a reinforced random walk model to describe the NP movements within the intravascular space of the tumor, which we approximate in a fixed two-dimensional (2D) circular-shaped domain. Tumor growth and death are neglected given the typical time scale of interest of 24–72 hours for NP transport to the tumor, much shorter than the tumor volume doubling time (e.g. for PDAC is 144 days according to [31]). We incorporate *intravascular* physiological traps that affect the residence of NPs in microvasculature into the 2D domain, including fenestrations and inter-endothelial gaps, and endothelium, while macrophages, despite functioning as traps in healthy tissues, constitute a part of the interstitial space of the tumor and are not considered as traps in the tumor domain [32]. We use published morphometric information (endothelial cell density, pore density) to populate the traps in the 2D domain. In the tumor, we impose intra-tumoral perfusion heterogeneity by discretizing the circular tumor into three zones: (i) vascularized $0.6R_t \leq r < R_t$, (ii) semi-

necrotic $0.1R_t \leq r < 0.6R_t$, and (iii) necrotic $r \leq 0.1R_t$, where r denotes the distance from the tumor center, and R_t is the radius of tumor [33] (see Fig. 2). Although NPs are confined to traverse the tumor region within the endothelial capillary walls, the diameter of a single capillary is below the spatial resolution of a tissue-scale model; instead the blood convection and the capillary tortuosity are respectively modeled by the deterministic and the stochastic parts of the reinforced random walk model, informed by the cell-scale sub-model.

To directly incorporate the one-to-one interaction between NPs and traps, we model the motion of individual NPs using an agent-based modeling (ABM) approach. NP motion is driven by a standard convection-diffusion process within the blood flow, microscopically represented by reinforced random walks. Thus, total NP motion in blood is governed by a mean convective velocity vector representing blood flow and the individual microscopic diffusive displacement for each NP, leading to the following stochastic differential equation (SDE) for each NP:

$$dX_t = u\,dt + \sqrt{2D}\,dW_t \tag{1}$$

where X_t is the nanovector jump length within time dt; u is the mean drift (in this case, velocity) vector; D is the diffusion coefficient of nanovectors; and W_t is the Wiener process. To numerically solve Eq. 1, we implement the Euler-Maruyama (EM) approximation in MATLAB™, which discretizes Eq. 1 as the following Markov chain:

$$X_{t+\Delta t} = X_t + u\,\Delta t + \sqrt{2D}\,\Delta W_t \tag{2}$$

where the increment ΔW_t is a normally distributed random variable with mean 0 and variance Δt [34].

III. Results and Discussion

The model was parameterized with data obtained from relevant published literature in cancer and physiology (e.g., [35]). We used the model to test the effect of NP physicochemical variables and physiological interventions on the efficiency of deployment of NPs to tumors.

We first used the model to simulate the injection of 1×10^{10} NPs 25 nm in diameter. As seen in Fig. 3, the whole-body scale analytical model predicts the NP concentration kinetics in different compartments, including free flowing NPs in systemic circulation, trapped NPs in liver, excreted NPs in kidneys, and trapped NPs in tumor. Since particle size in this case is above the cutoff for kidney clearance, we do not allow excretion through the renal route. In Fig. 3, we also plot numerical predictions for NP concentration delivered to the tumor by the tissue scale model (pink dots), which is consistent with the predictions of the whole-body system scale analytical model (pink dashed line), validating mathematically that the additional tissue and cell scale sub-models generate results consistent with the whole-body scale PBPK model.

To understand how NPs spatially accumulate in and around tumor tissues over time, we examined simulation results of the tissue-scale SDE model in the 2D tumor domain. As seen in Fig. 4, for a 10 mm diameter tumor, more NPs are trapped in the outer well-perfused

tumor region than the inner semi-necrotic domain. This can be attributed to the greater vasculature density and total number of traps in the outer region, resulting in a higher tendency for NPs to become trapped in the outer zone. Over time, the density of trapped NPs continues to increase, with more particles in the outer region than the inner region; that is, the trapped fraction (ratio of trapped NPs to the total NPs that entered the tumor in 1200 seconds) decreases from periphery to core at all times $t > 0$ in the model simulations. There are no NPs entrapped in the necrotic tumor core due to absence of vasculature, hence absence of traps.

In our multiscale approach, we used NP interactions with cellular scale traps (endothelium, pores, and macrophages) to determine the global biodistribution of NPs in systemic circulation and other critical regions of interest. While the analytical model determined the temporal kinetics of NP concentration in different regions of interest, the numerical model helped us understand the spatial distribution of NPs in the target site. In the future, we plan to incorporate the extravascular interstitial space into the current version of our model, and extend the model to a 3D domain, which requires more efficient schemes to improve the numerical performance.

Acknowledgment

We thank JR Ramirez, S Goel (Houston Methodist Research Institute), EJ Koay (MD Anderson Cancer Center), BM Wheeler, TA Brocato, and D Gupta (University of New Mexico) for helpful scientific discussions.

* This work has been supported in part by the National Science Foundation Grant DMS-1716737 (VC, ZW), the National Institutes of Health (NIH) Grants 1U01CA196403 (V.C., Z.W.), 1U01CA213759 (V.C., Z.W.), 1R01CA226537 (V.C., Z.W.), 1R01CA222007 (V.C., Z.W.), and U54CA210181 (V.C., Z.W.).

References

[1]. Tannock IF, Lee CM, Tunggal JK et al., “Limited penetration of anticancer drugs through tumor tissue a potential cause of resistance of solid tumors to chemotherapy,” Clinical cancer research, vol. 8, no. 3, pp. 878–884, 2002. [PubMed: 11895922]

[2]. Brocato T, Dogra P, Koay EJ et al., “Understanding Drug Resistance in Breast Cancer with Mathematical Oncology,” Current breast cancer reports, pp. 1–11, 2014.

[3]. Ashton S, Song YH, Nolan J et al., “Aurora kinase inhibitor nanoparticles target tumors with favorable therapeutic index in vivo,” Science translational medicine, vol. 8, no. 325, pp. 325ra17, 2016.

[4]. Maeda H, Wu J, Sawa T et al., “Tumor vascular permeability and the EPR effect in macromolecular therapeutics: a review,” Journal of Controlled Release, vol. 65, no. 1, pp. 271–284, 2000. [PubMed: 10699287]

[5]. Hosoya H, Dobroff AS, Driessen WHP et al., “Integrated nanotechnology platform for tumor-targeted multimodal imaging and therapeutic cargo release,” Proceedings of the National Academy of Sciences, vol. 113, no. 7, pp. 1877–1882, 2016.

[6]. Shi J, Kantoff PW, Wooster R et al., “Cancer nanomedicine: progress, challenges and opportunities,” Nature reviews cancer, 2016.

[7]. Wilhelm S, Tavares AJ, Dai Q et al., “Analysis of nanoparticle delivery to tumours,” Nature Reviews Materials, vol. 1, pp. 16014, 2016.

[8]. Sarin H, “Physiologic upper limits of pore size of different blood capillary types and another perspective on the dual pore theory of microvascular permeability,” J Angiogenes Res, pp. 2:14, 2010.

[9]. Dogra P, Adolphi NL, Wang Z et al., "Establishing the effects of mesoporous silica nanoparticle properties on in vivo disposition using imaging-based pharmacokinetics," Nat Commun, vol. 9, no. 1, pp. 4551, 10 31, 2018. [PubMed: 30382084]

[10]. Deisboeck TS, Wang Z, Macklin P et al., "Multiscale cancer modeling," Annu Rev Biomed Eng, vol. 13, pp. 127–55, 8 15, 2011. [PubMed: 21529163]

[11]. Wang Z, Butner JD, Kerketta R et al., "Simulating cancer growth with multiscale agent-based modeling," Semin Cancer Biol, vol. 30, pp. 70–8, 2, 2015. [PubMed: 24793698]

[12]. Cristini V, Koay E, and Wang Z, An Introduction to Physical Oncology: How Mechanistic Mathematical Modeling Can Improve Cancer Therapy Outcomes: CRC Press, 2017.

[13]. Wang Z, Kerketta R, Chuang YL et al., "Theory and Experimental Validation of a Spatio-temporal Model of Chemotherapy Transport to Enhance Tumor Cell Kill," PLoS Comput Biol, vol. 12, no. 6, pp. e1004969, 6, 2016. [PubMed: 27286441]

[14]. Wang Z, Deisboeck TS, and Cristini V, "Development of a sampling-based global sensitivity analysis workflow for multiscale computational cancer models," IET Syst Biol, vol. 8, no. 5, pp. 191–7, 10, 2014. [PubMed: 25257020]

[15]. Wang Z, Butner JD, Cristini V et al., "Integrated PK-PD and agent-based modeling in oncology," J Pharmacokinet Pharmacodyn, vol. 42, no. 2, pp. 179–89, 4, 2015. [PubMed: 25588379]

[16]. Das H, Wang Z, Niazi MK et al., "Impact of diffusion barriers to small cytotoxic molecules on the efficacy of immunotherapy in breast cancer," PLoS One, vol. 8, no. 4, pp. e61398, 2013. [PubMed: 23620747]

[17]. Pascal J, Ashley CE, Wang Z et al., "Mechanistic modeling identifies drug-uptake history as predictor of tumor drug resistance and nano-carrier-mediated response," ACS nano, vol. 7, no. 12, pp. 11174–11182, 2013. [PubMed: 24187963]

[18]. Pascal J, Bearer EL, Wang Z et al., "Mechanistic patient-specific predictive correlation of tumor drug response with microenvironment and perfusion measurements," Proc Natl Acad Sci U S A, vol. 110, no. 35, pp. 14266–71, 8 27, 2013. [PubMed: 23940372]

[19]. Frieboes HB, Smith BR, Wang Z et al., "Predictive Modeling of Drug Response in Non-Hodgkin's Lymphoma," PLoS One, vol. 10, no. 6, pp. e0129433, 2015. [PubMed: 26061425]

[20]. Brocato TA, Coker EN, Durfee PN et al., "Understanding the Connection between Nanoparticle Uptake and Cancer Treatment Efficacy using Mathematical Modeling," Sci Rep, vol. 8, no. 1, pp. 7538, 5 24, 2018. [PubMed: 29795392]

[21]. Brocato TA, Brown-Glaberman U, Wang Z et al., "Predicting breast cancer response to neoadjuvant chemotherapy based on tumor vascular features in needle biopsies," JCI Insight, vol. 5, 3 5, 2019.

[22]. Wang Z, and Deisboeck TS, "Mathematical modeling in cancer drug discovery," Drug Discov Today, vol. 19, no. 2, pp. 145–50, 2, 2014. [PubMed: 23831857]

[23]. Wang Z, and Deisboeck TS, "Dynamic Targeting in Cancer Treatment," Front Physiol, vol. 10, pp. 96, 2019. [PubMed: 30890944]

[24]. Dogra P, Butner JD, Y.-l. Chuang et al., "Mathematical modeling in cancer nanomedicine: a review," Biomedical Microdevices, vol. 21, no. 2, pp. 40, 4 04, 2019. [PubMed: 30949850]

[25]. Lunov O, Zablotskii V, Syrovets T et al., "Modeling receptor-mediated endocytosis of polymer-functionalized iron oxide nanoparticles by human macrophages," Biomaterials, vol. 32, no. 2, pp. 547–555, 2011. [PubMed: 20880574]

[26]. Carboni E, Tschudi K, Nam J et al., "Particle margination and its implications on intravenous anticancer drug delivery," AAPS PharmSciTech, vol. 15, no. 3, pp. 762–771, 2014. [PubMed: 24687242]

[27]. Stylianopoulos T, Diop-Frimpong B, Munn LL et al., "Diffusion anisotropy in collagen gels and tumors: the effect of fiber network orientation," Biophysical journal, vol. 99, no. 10, pp. 3119–3128, 2010. [PubMed: 21081058]

[28]. Bachler G, von Goetz N, and Hungerbühler K, "A physiologically based pharmacokinetic model for ionic silver and silver nanoparticles," International journal of nanomedicine, vol. 8, pp. 3365, 2013. [PubMed: 24039420]

[29]. Li D, Johanson G, Emond C et al., “Physiologically based pharmacokinetic modeling of polyethylene glycol-coated polyacrylamide nanoparticles in rats,” Nanotoxicology, no. 0, pp. 1–10, 2013.

[30]. Jones HM, and Rowland-Yeo K, “Basic concepts in physiologically based pharmacokinetic modeling in drug discovery and development,” CPT: pharmacometrics & systems pharmacology, vol. 2, no. 8, pp. e63, 2013. [PubMed: 23945604]

[31]. Furukawa H, Iwata R, and Moriyama N, “Growth rate of pancreatic adenocarcinoma: initial clinical experience,” Pancreas, vol. 22, no. 4, pp. 366–369, 2001. [PubMed: 11345136]

[32]. Gajewski TF, Schreiber H, and Fu Y-X, “Innate and adaptive immune cells in the tumor microenvironment,” Nature immunology, vol. 14, no. 10, pp. 1014, 2013. [PubMed: 24048123]

[33]. Wu J, Xu S, Long Q et al., “Coupled modeling of blood perfusion in intravascular, interstitial spaces in tumor microvasculature,” Journal of Biomechanics, vol. 41, no. 5, pp. 996–1004, 2008. [PubMed: 18222455]

[34]. Szymczak P, and Ladd AJC, “Stochastic boundary conditions to the convection-diffusion equation including chemical reactions at solid surfaces,” Physical Review E, vol. 69, no. 3, pp. 036704, 2004.

[35]. Simionescu M, Simionescu N, and Palade GE, “Morphometric data on the endothelium of blood capillaries,” The Journal of cell biology, vol. 60, no. 1, pp. 128–152, 1974. [PubMed: 4129076]

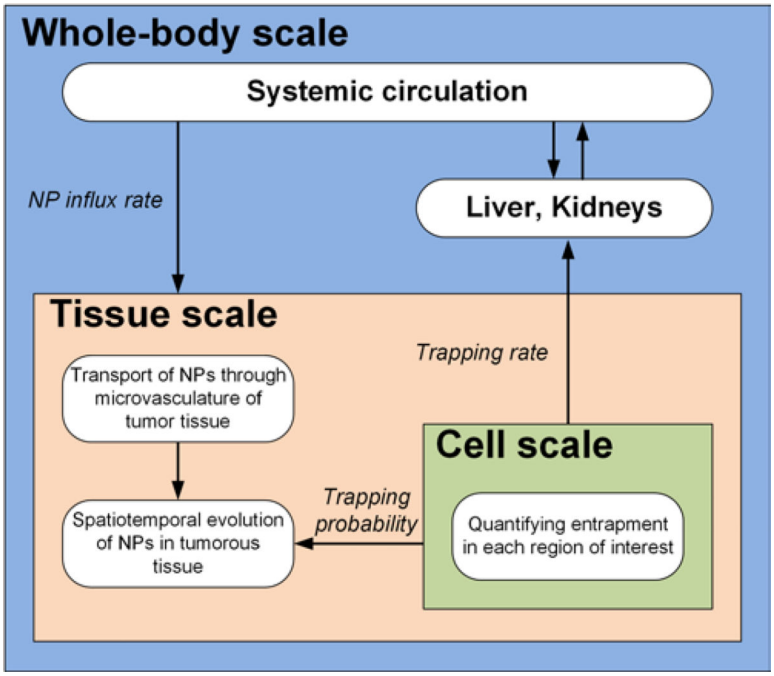

Fig. 1.

A schematic of key components and system interactions of the multiscale model. The model consists of three explicitly linked sub-models that operate at the whole-body, tissue, and cell scales, respectively. The whole-body scale model is a minimal PBPK model that determines the systemic temporal profile of NP concentration, which serves as an input for the tissue scale model in the form of influx rate of NPs into the host organ and tumor. In the tissue scale model, we simulate the transport of NPs through an abstractly represented intravascular space of tumor microvasculature and predict the spatiotemporal evolution of sequestered NPs to study delivery of nanomedicine to tumor. The model on the cell scale supplies the microscopic trapping rate for the whole-body scale PBPK model and trapping probability for the tissue scale model.

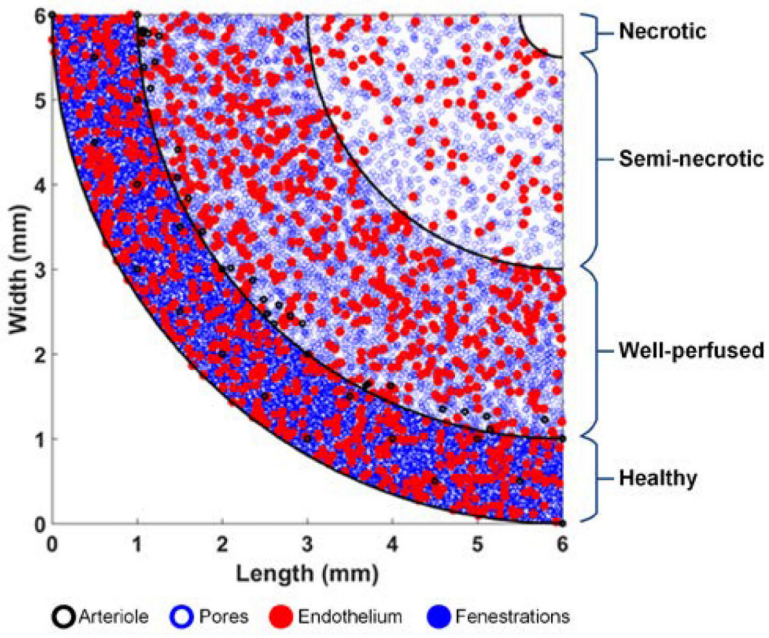

Fig. 2.

Simulation domain. For computational efficiency and statistically without losing generality, we simulate a quadrant of the circular tumor and assume symmetry for the other three. The tumor region is discretized into an outer well-perfused zone, middle semi-necrotic zone, and an inner necrotic tumor core. Only for visual comparison, an outermost healthy tissue zone is also shown in the snapshot, although it does not constitute a part of the simulated domain.

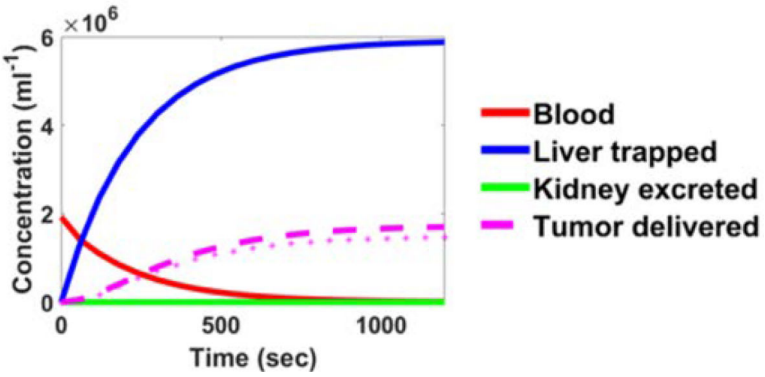

Fig. 3.

Model predictions of NP concentration over time. The predictions of concentration kinetics from the whole-body scale analytical model are shown for free-flowing NPs in systemic blood pool, trapped NPs in liver, excreted NPs from kidney, and trapped NPs in tumor. The numerical predictions (dotted pink) for tumor trapped NPs from the tissue scale model are also plotted, showing a consensus between different scales.

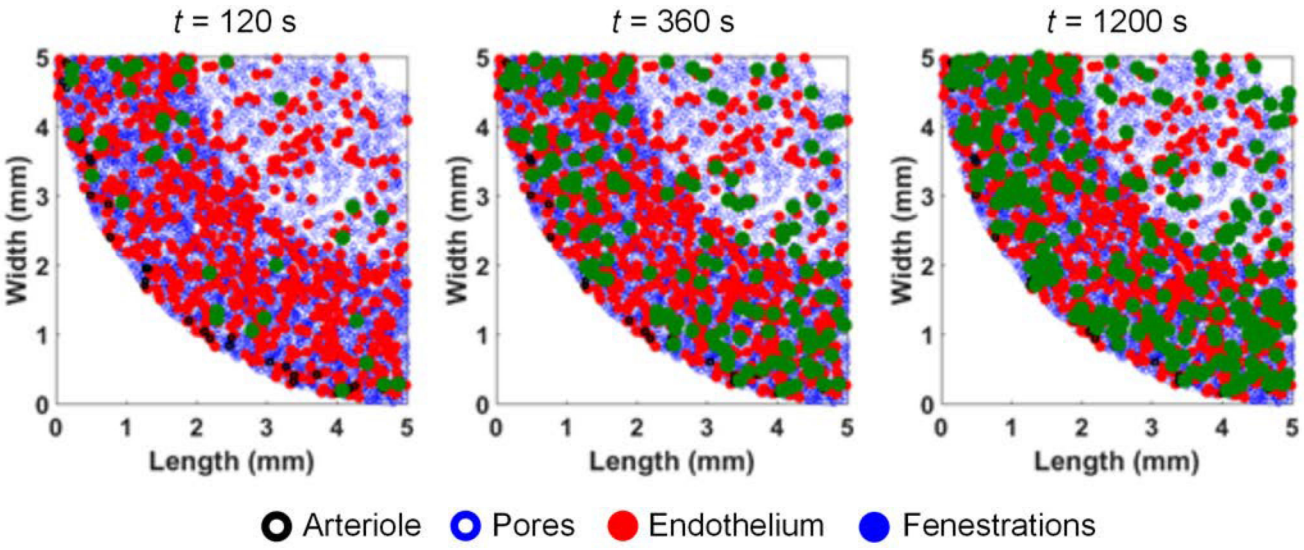

Fig. 4.

Tissue scale model simulations. Snapshots at 120, 360, and 1200 seconds are shown for a simulation of 25 nm diameter nanoparticles. The number of trapped NPs in the tumor domain increases over time. NPs are represented by solid green circles.